Integration of Self-Assembled Redox Molecules in Flash Memory Devices

Jonathan Shaw, Yu-Wu Zhong, Kevin J. Hughes, Tuo-Hung Hou, Hassan Raza, *Member, IEEE*, Shantanu Rajwade, Julie Bellfy, James R. Engstrom, Héctor D. Abruña, and Edwin Chihchuan Kan, *Senior Member, IEEE*

***Abstract*—Self-assembled monolayers (SAMs) of either ferrocenecarboxylic acid or 5-(4-Carboxyphenyl)-10,15,20-triphenylporphyrin-Co(II) (CoP) with a high-κ dielectric were integrated into the Flash memory gate stack. The molecular reduction–oxidation (redox) states are used as charge storage nodes to reduce charging energy and memory window variations. Through the program/erase operations over tunneling barriers, the device structure also provides a unique capability to measure the redox energy without strong orbital hybridization of metal electrodes in direct contact. Asymmetric charge injection behavior was observed, which can be attributed to the Fermi-level pinning between the molecules and the high-κ dielectric. With increasing redox molecule density in the SAM, the memory window exhibits a saturation trend. Three programmable molecular orbital states, i.e., CoP^{0}, CoP^{1-}, and CoP^{2-}, can be experimentally observed through a charge-based nonvolatile memory structure at room temperature. The electrostatics is determined by the alignment between the highest occupied or the lowest unoccupied molecular orbital (HOMO or LUMO, respectively) energy levels and the charge neutrality level of the surrounding dielectric. Engineering the HOMO–LUMO gap with different redox molecules can potentially realize a multibit memory cell with less variation.**

***Index Terms*—Coulomb blockade effect, high-κ dielectric, nonvolatile memory devices, reduction–oxidation (redox)-active molecules, self-assembled monolayer (SAM).**

I. Introduction

FLASH memory device structures with discrete charge storage such as nanocrystals (NCs) and dielectric traps are potential candidates for continuous memory scaling by maintaining a coupling ratio and reducing crosstalk in conventional floating-gate devices. A metal NC embedded in a high-κ dielectric [1] has been proposed to improve low-voltage program/erase (P/E) efficiency by the 3-D field enhancement effect [2]. The metal work function also provides an additional offset to the Si band edges to prolong retention. However, nonuniformity in NC size and density raises concerns of the parametric yield for aggressive scaling [3], [4]. Charge storage in dielectric traps is also vulnerable to trap density and energy variations.

In comparison, a combination of the top-down lithography and the bottom-up molecule self-assembly processes can offer a uniform charge density and possible stable multilevel storage in a single memory cell [5]. The monodisperse nature of the molecular orbitals (MOs) can potentially reduce cell variations, whereas the distinct energy levels may enable stepwise charging for precise control of each memory state. By attaching reduction–oxidation (redox) molecules as a floating gate in the complementary metal–oxide–semiconductor (CMOS) structure, one also creates a high-impedance nonamperometric electrode for probing the molecular redox states, in contrast to the low-impedance connections used in cyclic voltammetry (CyV) [6]–[9]. Previous studies have shown capacitance and conductance peaks associated with the charging and the discharging of the carriers stored at the MOs [7] and CyV hysteresis owing to the redox of molecules attached to the SiO_2 surface [6], [8], [9].

Compared with the CyV measurements, where the insulating barrier was only deposited on one side [6], [9], the new structure provides insulating barriers above and below the molecules, which further lessen the possibility of orbital hybridization from the gate. A strong coupling between the electrode and the molecule may lead to molecule-independent switching behavior and modification of the intrinsic spacing of the energy levels [10], which makes it difficult to study the molecule-specific behaviors. Furthermore, the lack of an insulating capping layer in CyV compromises carrier retention. An additional shortcoming with the CyV method is the slow timescale due to its reliance on ionic movement. The operation speed can be enhanced significantly with an all-electron conduction mechanism in the proposed structure. Furthermore, the specifically tailored redox molecules can be self-assembled as a monolayer in current CMOS technology through the chosen functional end group, where the discrete levels of the MOs can be preserved as discrete memory states.

In this paper, we have integrated various molecules with a high-κ dielectric in an otherwise standard Flash memory gate stack. We report the charge retention and P/E characteristics. We further confirm that porphyrin molecules have the thermal budget that can withstand postmetal gate annealing [11]—an important requirement for CMOS compatibility. Compared with the previous studies [6]–[9], we were able to confirm an interaction with multiple states of redox-active molecules, instead of interface traps.

Manuscript received May 28, 2010; revised November 18, 2010; accepted November 25, 2010. Date of publication December 30, 2010; date of current version February 24, 2011. This work was supported by the National Science Foundation through the Cornell Center of Materials Research Interdisciplinary Research Group on Controlling Electrons at the Interface. The review of this paper was arranged by Editor Y.-H. Shih.

J. Shaw, S. Rajwade, H. D. Abruña, and E. C. Kan are with the School of Electrical and Computer Engineering, Cornell University, Ithaca, NY 14853 USA (e-mail: jts57@cornell.edu).

Y.-W. Zhong is with the Laboratory of Photochemistry, Institute of Chemistry, Chinese Academy of Sciences, Beijing 100864, China.

K. J. Hughes and J. R. Engstrom are with the School of Chemical and Biomolecular Engineering, Cornell University, Ithaca, NY 14853 USA.

T.-H. Hou is with the School of Electrical and Computer Engineering, National Chiao Tung University, Hsinchu 300, Taiwan.

H. Raza is with the College of Engineering, University of Iowa, Iowa City, IA 52242 USA.

J. Bellfy is with Villanova University, Villanova, PA 19085 USA.

Digital Object Identifier 10.1109/TED.2010.2097266

0018-9383/$26.00 © 2010 IEEE

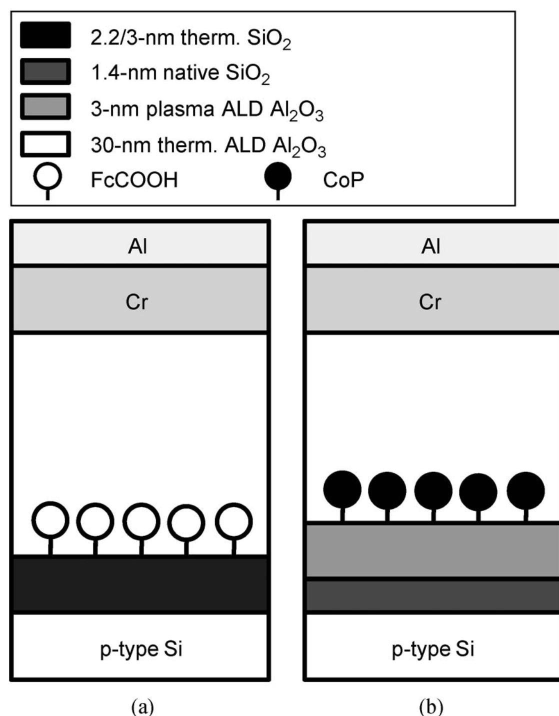

Fig. 1. Schematics of the MOS capacitor structure with (a) FcCOOH (S1) and (b) CoP (S2) molecules integrated as storage nodes.

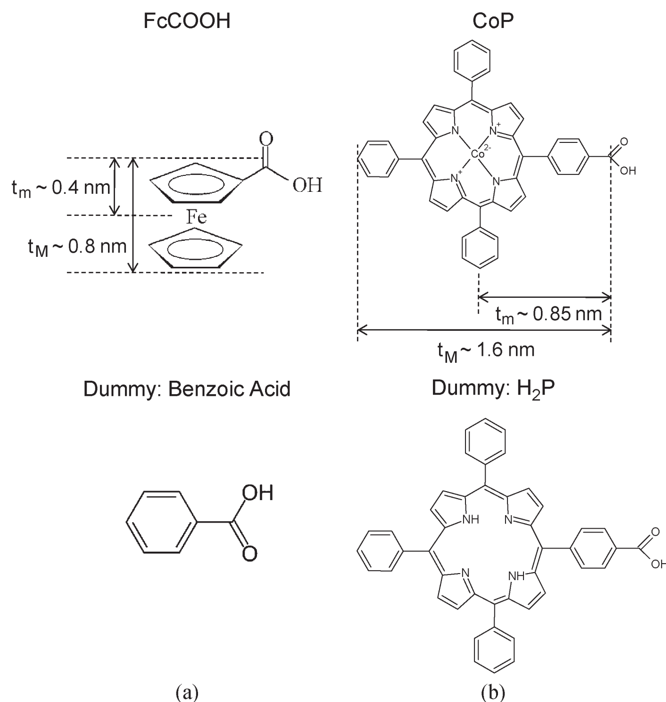

Fig. 2. Molecular structure of FcCOOH, CoP, and the respective dummy molecules used to control surface coverage density of the redox-active molecules. The approximate distance from the attachment site to the central transition metal t_m and the thickness as-deposited on the surface t_M are illustrated for each redox-active molecule.

II. Device Fabrication

The metal–oxide–semiconductor (MOS) capacitor structure, similar to that used in Flash memory devices [12], [13], with redox molecules embedded in the control dielectric, was fabricated. Two types of redox molecules were integrated: ferrocenecarboxylic acid (FcCOOH) and 5-(4-Carboxyphenyl)-10,15,20-triphenyl-porphyrin-Co(II) (CoP). The schematics of the devices with FcCOOH (S1) and CoP (S2) molecules are illustrated in Fig. 1. Both molecules are stable in air, with FcCOOH and CoP exhibiting two and three stable redox states, respectively.

We followed a self-assembled monolayer (SAM) formation process similar to previous literature [9], utilizing the carboxyl functional group on the OH-terminated surface. For S1, after 2.2- or 3.0-nm dry thermal oxide growths on a p-Si(100) substrate, the wafer was immersed in a solution of dimethyl formamide (DMF) with 1-mM FcCOOH. The solution was kept at 80 °C for 120 min under an argon environment during the self-assembly process. For S2, the wafer was first placed in a 1% hydrofluoric acid (HF) solution to remove the native oxide, followed with deionized (DI) water rinse/N_2 blow dry, and then immediately loaded into the atomic layer deposition (ALD) chamber. After 3 nm of Al_2O_3, the wafer was immersed in a 1-mM CoP solution of DMF at room temperature for 24 h under an argon environment. It is worthwhile to note that native SiO_2 forms readily in air. A native oxide of ~1 nm was present before Al_2O_3 growth on a separate test sample, which went through an identical HF etch process, measured by ellipsometry. Prior to the growth of the control dielectric, the native SiO_2 was measured to be ~1.4 nm on our test sample with no molecules present. The native SiO_2 possibly formed during DI water rinse/N_2 dry after etching by HF and the initial cycles of thermal Al_2O_3 deposition. The surface density has been estimated to be around 1×10^{14} and 0.45×10^{14} cm^{-2} for FcCOOH and CoP SAMs, respectively [6], assuming a full surface coverage. Furthermore, the thickness values of FcCOOH and CoP SAMs measured by ellipsometry were in the range of 0.9–1.2 and 1.5–1.6 nm, respectively, which is in good agreement with a previous estimate where the thickness is estimated to be 0.8 and 1.5 nm by impedance spectroscopy [8]. After the self-assembly process, DMF was used to rinse the wafer to remove any residual molecule that is not covalently bonded to the surface. The SAM was covered by 30 nm of ALD Al_2O_3 grown by the reaction of trimethylaluminum and H_2O at 110 °C. The Cr/Al control gate was then deposited and patterned, followed by a H_2/N_2 forming gas anneal at various conditions.

We report the molecular structure of FcCOOH and CoP molecules in Fig. 2. t_m is the approximate distance from the attachment site to the redox-active transition metal, whereas t_M is the thickness of the molecule. The dummy molecules, exhibiting no redox states, were added in the control splits for various surface density coverage of the redox-active molecules. Dummy molecules were selected based on structural similarity to the *active* molecules to ensure solubility of the dummy molecule in the deposition solution and to promote effective mixing of the dummy and active molecules on the surface. The dummy molecule for FcCOOH is benzoic acid (Bz), where $1:100$ mixing is derived from 0.01 mM of FcCOOH and 1 mM of Bz. Assuming the $1:100$ mixing ratio in the bulk solution leads to a $1:100$ mixing of FcCOOH:Bz on the attachment surface, the density corresponds to an intermolecule spacing of ~5.8 nm for

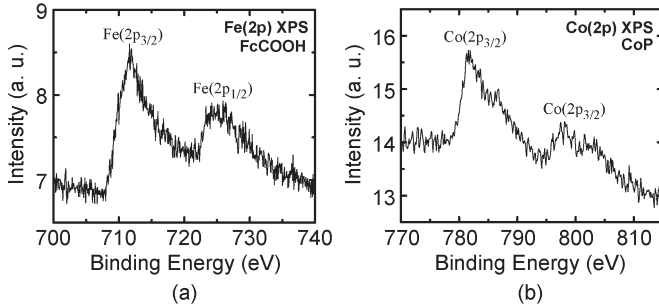

Fig. 3. XPS data of the (a) FcCOOH SAM deposited on thermally grown SiO_2 and (b) CoP SAM deposited on Al_2O_3 ALD. For XPS studies, no dummy molecules were used for preparing the SAM solution. The SAM solution concentration of FcCOOH and CoP is 1 mM.

FcCOOH. We estimate the minimum intermolecule distance of a 0.1-eV Coulomb blockade as

$$\Delta E = \frac{1}{4\pi\varepsilon_r\varepsilon_0}\frac{q_1 q_2}{r} \leq 0.1 \text{ eV}, \qquad r \geq 5.75 \text{ nm} \tag{1}$$

where ΔE is the energy shift due to repulsion force from the neighbor molecules, q_1 and q_2 are the charges stored in the redox-active molecules, r is the intermolecule distance, and ε_r and ε_0 are the relative and vacuum permittivities. Here, we assume the ε_r of Bz to be 2.5. CoP was mixed with 5-(4-Carboxyphenyl)-10,15,20-triphenyl-21,23H-porphyrin (H_2P), which acts as the dummy molecule, at a 1:20 ratio.

III. Results and Discussion

Fig. 3 shows the X-ray photoelectron spectroscopy (XPS) measurement on the samples of as-deposited FcCOOH and CoP SAMs. The $2p_{1/2}$ and $2p_{3/2}$ electron configurations corresponding to the orbital binding energy peaks of iron and cobalt can be clearly observed for the FcCOOH and CoP SAMs, respectively. Since ferrocene is an organometallic compound that contains two cyclopentadienyl rings bound to a central iron, the observation of peaks at binding energy levels characteristic of the Fe $2p_{1/2}$ and $2p_{3/2}$ levels is evidence of ferrocene on the tunneling oxide. Similarly, in the case of the CoP SAM, the characteristic cobalt binding energy peaks indicate the existence of CoP deposited on the Al_2O_3 surface.

The XPS features may be also used to estimate the absolute densities of the redox-active molecules [14]. To quantify the coverage density of the redox molecules chemisorbed to the oxide surfaces, we use X-ray photoelectron spectra from the evaporated Au (not shown) on a silicon substrate as a reference standard. The integrated intensity under the [Au(4f)] feature from the standard is proportional to $\sigma_{\mathrm{Au}} N_{\mathrm{Au}} \lambda_{\mathrm{Au}} T(E_{\mathrm{Au}})$, where σ_{Au}, $N_{\mathrm{Au}} = 5.88 \times 10^{22}$ atoms/cm^3 [15], $\lambda_{\mathrm{Au}} =$ 1.78 nm [16], and $T(E_{\mathrm{Au}})$ are the photoelectron cross section, atomic density, inelastic mean free path, and analyzer transmission, respectively, which is inversely proportional to the photoelectron kinetic energy. If we assume that the redox molecules form a finite thickness monolayer on the surface d_{SAM} with the atomic density N_{SAM}, and $d_{\mathrm{SAM}} \ll$ inelastic mean free path of SAMλ_{SAM}, the area under the Fe(2p) and Co(2p) features will then be proportional to $\sigma_{\mathrm{Fe}} N_{\mathrm{SAM}} d_{\mathrm{SAM}} T(E_{\mathrm{Fe}})/\cos\theta$ and $\sigma_{\mathrm{Co}} N_{\mathrm{SAM}} d_{\mathrm{SAM}} T(E_{\mathrm{Co}})/\cos\theta$, where $\sigma_{\mathrm{Au}}/\sigma_{\mathrm{Fe}} \sim 1.04$ and $\sigma_{\mathrm{Au}}/\sigma_{\mathrm{Co}} \sim 0.89$ [17] are for Fe(2p) and Co(2p), respectively, and $\theta = 55^\circ$ is the photoelectron takeoff angle from the surface normal. With these assumptions, the surface density $N_{\mathrm{SAM}} d_{\mathrm{SAM}}$ (in molecules per square centimeter) of FcCOOH and CoP can then be calculated as 1.58×10^{14} and 3.6×10^{13} molecules/cm^2, respectively, for SAMs undiluted with dummy molecules, which agree well with previous estimation by CyV [6]. Considering the assumptions that were made with the estimation method and the background noise, the absolute accuracy is approximately $\pm 35\%$.

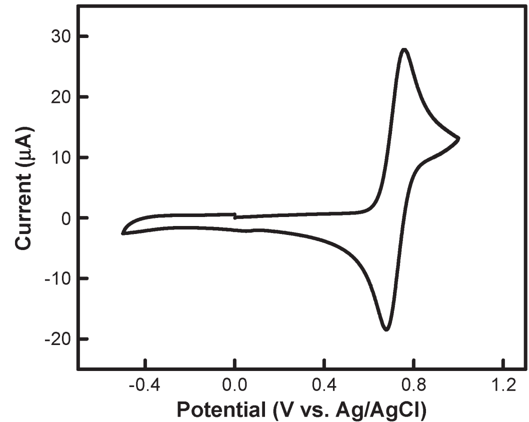

Fig. 4. CyV of 2-mM FcCOOH in acetonitrile containing 0.1-M $TBAPF_6$ as a supporting electrolyte. Ag/AgCl was used as the reference electrode.

Furthermore, the contact angles measured before and after FcCOOH attachment were 10° and 80°, respectively, which indicates that the film went from a hydrophilic oxide to a more hydrophobic organic surface. For CoP, the contact angles were 31° and 55° before and after the self-assembly process, respectively. Our results from XPS, ellipsometry, and contact angle measurements suggest that a monolayer of FcCOOH and CoP molecules was formed on the SiO_2 and Al_2O_3 surfaces, respectively. Furthermore, CyV was performed with 2 mM of FcCOOH in acetonitrile containing 0.1 M of tetrabutylammonium hexafluophosphate ($TBAPF_6$) as a supporting electrolyte, as illustrated in Fig. 4. The current peaks are associated with the oxidation (negative current) and the reduction (positive current) of the molecules. One reversible redox state was observed at +0.71 V versus the Ag/AgCl reference electrode.

Apart from this, from the resonant peak in the ultraviolet/visible light (UV/Vis) absorption spectrum shown in Fig. 5, the HOMO–LUMO energy gap can be estimated by the de Broglie equation $E = hc/\lambda$, where c is the speed of light in a vacuum, and E is the energy gap that corresponds to the resonant wavelength λ. The spectroscopic HOMO–LUMO energy gap was estimated to be ∼2.8 and ∼2.65 eV for FcCOOH and CoP molecules, respectively, which matches well with the *ab initio* calculations by the density functional theory (DFT) [18], [19]. The HOMO–LUMO energy levels are estimated by the DFT to be about −4.51/−1.72 eV for the FcCOOH molecule and −4.8/−2.2 eV for the CoP molecule [18], [19].

Consider the electrical characterization of the FeCOOH sample, for which the high-frequency capacitance–voltage (HFCV) measurements in Fig. 6(a) were taken by applying stress

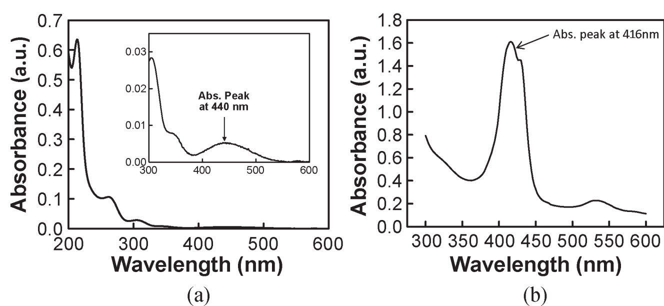

Fig. 5. UV/Vis absorption spectrum of (a) FcCOOH in acetonitrile and (b) CoP in DMF. Deduced from the maximum absorption peak of the lowest energy band at 440 nm, the spectroscopic HOMO–LUMO energy gaps are estimated to be ∼2.8 and ∼2.65 eV for FcCOOH and CoP molecules, respectively.

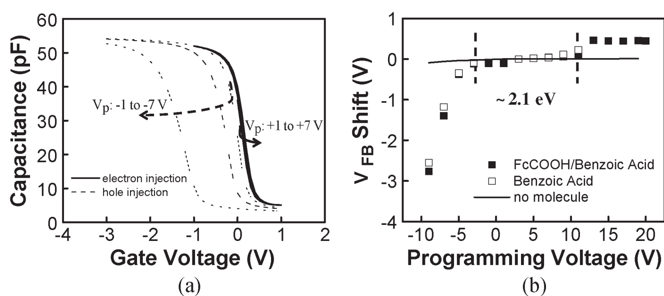

Fig. 6. (a) HFCV measurements and (b) ΔV_{FB} as a function of the programming voltage at 10 K and room temperature for capacitors with FcCOOH molecules. The mixture between FcCOOH and Bz has a 1 : 100 ratio. The device was annealed at 400 °C for 30 min. Carrier injection tests were carried out by applying stress voltages for 5 s before each CV sweep. The programming voltage V_p for electron and hole charging is applied from ±1 to ±7 V in a 2-V increment. Subsequently, the gate voltage is swept from accumulation to inversion for electron charging and inversion to accumulation for hole charging. The size of the MOS capacitor is 150 × 150 μm^2.

voltages on the control gate for 5 s to ensure that the program operation reaches the steady state, followed by sweeping the voltage from positive to negative direction for studying electron injection and from negative to positive direction for hole injection from the silicon substrate. All subsequent HFCV measurements performed at 10 K were under a light source to promote minority carrier generation. For this sample, 2.2 nm of thermal oxide was grown as the tunneling oxide with a forming gas anneal performed at 400 °C for 30 min. The surface coverage ratio is assumed to be identical to the bulk solution ratio of 1 : 100 between FcCOOH and Bz (as a dummy molecule). First, we notice that, at small programming voltages, hole injection showed a large memory window, whereas electron injection is negligible, which indicates that hole injection is preferred when a FcCOOH SAM is embedded in Al_2O_3. Also worth noticing is the CV stretch-out at higher programming voltages, which can be attributed to charge leakage back to the silicon substrate. Fig. 6(b) shows the amount of flatband shift ΔV_{FB} as a function of the programming voltage extracted from the HFCV measurements. The participation of both electrons and holes is evident from the linear increase in ΔV_{FB} by positive and negative writing conditions, respectively.

The injected charges have three possible storage sites: 1) dielectric traps of Al_2O_3; 2) traps near the Al_2O_3/FcCOOH interface; and 3) FcCOOH itself to reduce/oxidize the molecule. Since the sample without any molecules embedded in the gate stack has shown negligible ΔV_{FB} for programming voltages of -10 to $+20$ V, charges are not likely to be stored in dielectric traps of Al_2O_3. A linear increase in ΔV_{FB} with respect to the programming voltage is an indication of charges being stored at the interface states, whereas a staircase behavior has been regarded as a signature of charge storage in the redox molecules, which has discrete energy levels corresponding to the various MOs [5]. Saturation at high positive biases can be a result of Frenkel–Poole (F–P) leakage through the control dielectric or the Coulomb blockade effect [5]. The charge neutrality level (CNL) of Al_2O_3 deposited by ALD is around -5.2 eV [20]. The CNL can be regarded as a local Fermi level of the interface states or metal-induced gap states [21], which are dangling bonds that disperse across the band gap of the dielectric. It is evident that the energy-level alignment between the MOs and the surrounding dielectric's CNL is crucial for determining the memory properties [5], [20], [21]. Coulomb staircase behavior at negative gate biases was not observed for several possible reasons: First, holes have a preference to relax to the CNL, which is slightly above the HOMO energy level. Second, upon interface formation, the energy level may have been shifted due to fractional charge transfer at the interface. Further evidence comes from the fact that the control sample with only Bz molecules also results in hole storage with a slightly smaller memory window than samples with FcCOOH molecules. Knowing that Bz molecules do not exhibit any redox states, injected holes are most likely stored in the interfacial traps created by the dangling bonds. This indicates that both FcCOOH and Bz molecules generate traps at the dielectric interface as one would expect, which are the preferential sites for hole storage.

Moreover, the preference for hole storage can be further explained by the Fermi-level pinning theory [5], [13], [22]. Fig. 7 illustrates the band diagram with an FcCOOH molecule as the storage node. Electron injection is forbidden at low programming voltages because electrons must have an energy greater than or equal to $E_{\mathrm{LUMO}} - E_c + \Delta E_{\mathrm{ch},e} = 2.35$ eV $+ \Delta E_{\mathrm{ch},e}$, where E_c is the silicon conduction band, and $\Delta E_{\mathrm{ch},e}$ is the single-electron charging energy. Upon injection, electrons would preferentially relax to the interface traps near the CNL with lower energy. From the energy alignment, the energy required for hole injection is $E_v - E_{\mathrm{HOMO}} + \Delta E_{\mathrm{ch},h} = -0.66$ eV $+ \Delta E_{\mathrm{ch},h}$, where E_v is the silicon valence band, and $\Delta E_{\mathrm{ch},h}$ is the single-hole charging energy. Thus, hole storage is energetically favorable than electron storage.

Apart from this, Fig. 8 illustrates the change in memory window for different mixture ratios between FcCOOH and Bz at negative gate biases. For this sample, the forming gas anneal was performed at 300 °C for 90 min with 3 nm of thermal SiO_2 as the tunneling oxide. The amount of ΔV_{FB} increases proportionally with the increase in the density of FcCOOH molecules in the SAM, which suggests that increasing the number of FcCOOH molecules increases the number of sites for hole storage. This also confirms our previous argument, derived from the energy band diagram, that holes have preference to be stored at interfacial trap sites created by FcCOOH molecules.

To pinpoint the cause of ΔV_{FB} saturation at positive gate biases and the charge storage mechanism, we decreased the density of FcCOOH molecules and performed HFCV

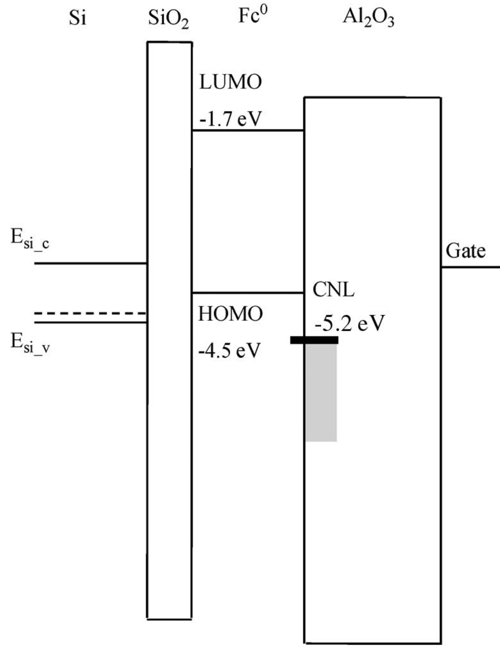

Fig. 7. Energy band diagram representation of the capacitor structure with FcCOOH molecules. The CNL of Al_2O_3 is shown, and the FcCOOH molecule is assumed to be in its neutral state.

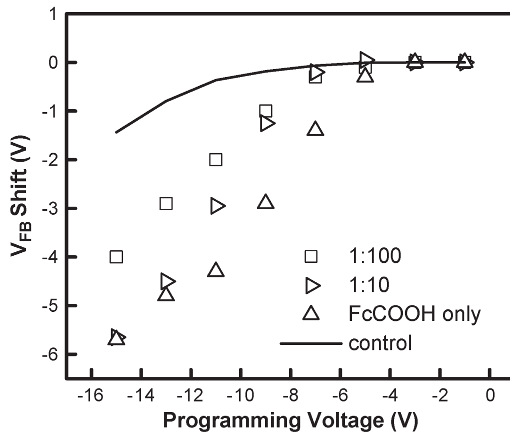

Fig. 8. ΔV_{FB} as a function of the programming voltage for devices with FcCOOH molecules mixed with Bz molecules at mixture ratios of 1 : 100, 1:10, and FcCOOH molecules only in the deposition solution. A 90-min forming gas anneal was performed at 300 °C. Measurements taken on the sample with no molecules are also shown for comparison.

measurements at cryogenic temperatures. A new batch of samples (with 3 nm of SiO_2 as the tunneling oxide) was annealed at 200 °C for 60 min, and the mixture ratios between FcCOOH and Bz molecules were 1 : 100 and 1 : 200 (e.g., 0.005 mM of FcCOOH to 1 mM of Bz), which translates to the intermolecular distance for FcCOOH of 5.8 and 8.2 nm, respectively, assuming that the surface coverage ratio is the same as the bulk solution for preparing the SAM. The concentration of FcCOOH molecules is reduced to moderate the Coulomb repulsion force, which could affect the charging potential of neighboring molecules. A lower annealing temperature was chosen to avoid molecule degradation.

In Fig. 9, HFCV and ΔV_{FB} as a function of the programming voltage are shown. In Fig. 9(a), we notice that asymmetric in-

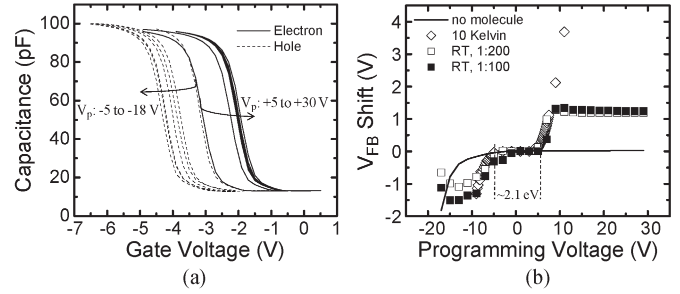

Fig. 9. (a) HFCV and (b) ΔV_{FB} as a function of the programming voltage at 10 K and room temperature for FcCOOH molecules. The two mixture ratios between FcCOOH and Bz molecules are 1 : 200 and 1 : 100 with a tunneling oxide of 3-nm thermal SiO_2. A 60-min forming gas anneal was performed at 200 °C. Measurements taken on the sample with no molecules are also shown for comparison. HFCV measurements were taken at 100 kHz. The programming voltage V_p for electron and hole charging is applied from $+5$ to $+30$ V and -5 to -18 V, respectively. Subsequently, the gate voltage is swept from accumulation to inversion for electron charging and inversion to accumulation for hole charging. The size of the MOS capacitor is $200 \times 200\ \mu\mathrm{m}^2$.

jection and CV stretch-out are no longer present, possibly due to interface dipole formation, which shifted the band alignment. At 10 K, the amount of ΔV_{FB} increases linearly in proportion to the positive gate biases, whereas a saturation behavior was observed at room temperature. In addition, the saturation voltage is approximately the same for the two different mixture ratios. Both the temperature and concentration dependences suggest that the saturation behavior originates from F–P conduction through the control dielectric at room temperature [5], which is a nonideal situation in our present process integration.

ΔV_{FB} can be described by the following relation:

$$\Delta V_{\mathrm{FB}} \approx \frac{Q}{C_{\mathrm{cont}}} \approx \frac{q \times n \times N}{C_{\mathrm{cont}}} \tag{2}$$

where Q, q, n, N, and C_{cont} are the total stored charge density in the molecules, the elemental charge, the number of charges per molecule, the number density of the molecule, and the capacitance of the control oxide, respectively. The ΔV_{FB} shift is approximately 1.3 V in Fig. 9, and from (2), we obtain a trap density of 2×10^{12} cm^{-2}. Once all the traps are occupied, any additional electron would need to overcome the repulsion force from the electrons stored in the lowest energy state of interface traps to enter the MO. As we increase the gate bias further, the electrons would gain enough energy against the repulsion force but tends to leak out of the control dielectric by F–P conduction.

There is one more interesting observation. Modeling the molecule as a thin dielectric layer, we can obtain the total voltage drop from the SiO_2/Si interface to the central redox-active atom V_{ch} as

$$V_{\mathrm{ch}} = \frac{t_{\mathrm{tunn}} + \frac{\varepsilon_{\mathrm{ox}}}{\varepsilon_M} t_m}{t_{\mathrm{tunn}} + \frac{\varepsilon_{\mathrm{ox}}}{\varepsilon_M} t_M + \frac{\varepsilon_{\mathrm{ox}}}{\varepsilon_{\mathrm{cont}}} t_{\mathrm{cont}}} V_G \tag{3}$$

where t_{tunn}, t_{cont}, and t_m are the tunnel oxide thickness (SiO_2), the physical thickness of the Al_2O_3 control dielectric, and the approximate distance from the attachment site to the redox-active transition metal, respectively, as illustrated in Fig. 2. t_m is estimated to be $0.5 t_M$. ε_M and t_M are the dielectric constant and the thickness of the molecule, respectively, assuming that the silicon channel is under inversion or

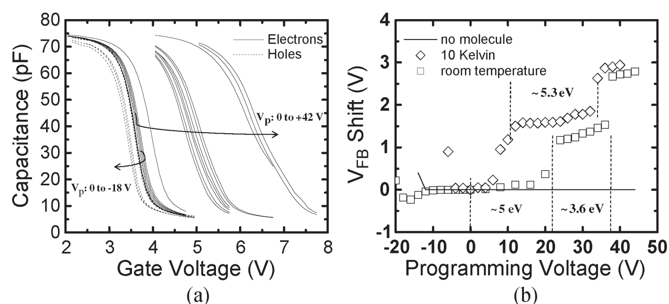

Fig. 10. (a) HFCV and (b) ΔV_{FB} as a function of the programming voltage at 10 K and room temperature for the device with CoP molecules. The mixture ratio between CoP and H_2P is 1 : 20. A 30-min forming gas anneal was performed at 400 °C. Measurements taken on the sample with no molecules are also shown for comparison. HFCV measurements were taken at 100 kHz. The programming voltage V_p for electron and hole charging is applied from 0 to +42 V and 0 to −18 V, respectively. Subsequently, the gate voltage is swept from accumulation to inversion for electron charging and inversion to accumulation for hole charging. The size of the MOS capacitor is 200 × 200 μm^2.

accumulation. ε_M and t_M were determined in previous reports through impedance characterization to be 2.4 and 0.8 nm, respectively [8]. $\varepsilon_{\mathrm{cont}} = 9$ and $\varepsilon_{\mathrm{ox}} = 3.9$ are the dielectric constants of the control and tunneling oxides, respectively. In Figs. 6(b) and 9(b), the total blockade voltage can be calculated using (3) to be 2.1 eV in both cases, assuming that the energy required to initiate charge injection is approximately the same as eV_{ch}, with a shift in the absolute value for different annealing conditions. The shift indicates that the slightly different band alignment is due to the interfacial dipoles and the fixed charge at the molecule/Al_2O_3 interface, but the HOMO–LUMO energy gap is identical in both cases. Depending on the annealing condition, the density of interface traps will vary as a function of energy, which leads to the difference in flatband voltage. However, the consistency in the blockade voltage suggests that the MO energy spacing is preserved within the dielectric environment.

If the molecule density is high enough to enable free lateral transport (continuous floating gate), ΔE_{ch} will not be significant, and the discrete energy levels of the molecule would not be observable. The dilute FcCOOH/Bz samples have a total blockade energy of 2.1 eV, which indicates that the charging energy remains negligible after diluting the concentration of FcCOOH molecules. Therefore, it is likely that the carriers were injected into the interfacial traps since significant trap states are involved at the FcCOOH/Al_2O_3 or the Bz/Al_2O_3 interface. The constant plateau regions suggest that the HOMO–LUMO energy gap acts as the energy barrier that carriers must overcome to initiate electron/hole injection. However, carriers quickly relax to surrounding interface states to favor the lower CNL energy.

Next, we consider the electrical characterization for the CoP redox-active molecules. Fig. 10(a) and (b) shows the HFCV and memory window as a function of the programming voltage, respectively. Gate injection prohibits hole injection beyond programming voltages below −18 V. On the contrary, electron injection shows two distinct levels of the Coulomb staircase, which is in good agreement with the previous measurements using CyV [6]–[9]. Assuming that full coverage density of 4.5 × 10^{13} cm^{-2} and 1:20 dilution of the deposition solution lead to

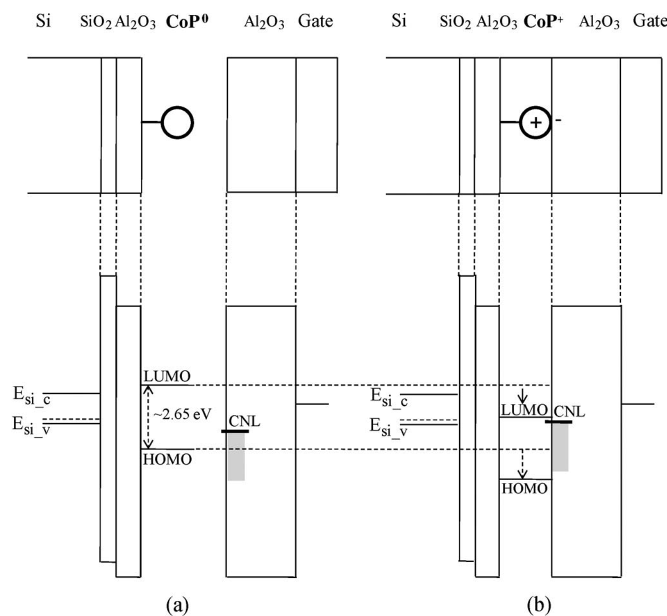

Fig. 11. Energy band diagram at thermal equilibrium states (a) before and (b) after a CoP molecule is in contact with the surrounding dielectric. The CNL and density of states are determined by the oxide's atomic configuration, which are sensitive to composition stoichiometries and deposition surface. The figure is not drawn to scale. The electron-filled interface states are indicated as the shaded regions. The HOMO–LUMO energy gap is estimated from the UV/Vis absorption spectra to be ∼2.65 eV.

equal dilution of the SAM, the 1:20 mixture ratio with H_2P translates to a CoP number density of about 2.2 × 10^{12} cm^{-2} and a flatband voltage shift of about 1.32 V for the single-electron injection. This value matches well with the amount of flatband voltage shift observed in Fig. 10, which is approximately 1.4 V at room temperature and 1.6 V at 10 K. At room temperature, the large leakage between the carrier storage sites and the gate, possibly through hopping, prevents efficient charging of CoP molecules. Contrarily, measurements that were taken at 10 K also show Coulomb staircase behavior, but carrier storage begins at lower programming voltages due to the elimination of F–P leakage. It is worthwhile to note that the initial flatband voltage is $\sim +3.5$ V, which differs from an ideal p-type MOS stack, which exhibits a flatband voltage of ~ -0.9 V. The difference in flatband voltage is from the large amount of fixed charge created at the molecule/Al_2O_3 interface due to the nonideal growth surface.

Fig. 11(a) and (b) illustrates the energy band diagrams before and after depositing Al_2O_3 as the control dielectric on top of the molecules, respectively. The HOMO–LUMO energy levels for neutral CoP^0 were estimated by DFT calculation [19], whereas the CNL of ALD Al_2O_3 is −5.2 eV. According to the HOMO–LUMO energy levels of CoP^0 and CNL, electrons have the energy preference to relax to the CNL, and the Coulomb staircase would not be observed before the control dielectric is deposited. On the other hand, the interface dipole formation at the CoP/Al_2O_3 interface can lead to a different thermal equilibrium state, likely a monocation (CoP^{1+}), established by hole transferring from the interface states into CoP^0. In addition, electron injection to the LUMO energy level is evident from the Coulomb staircase. Therefore, we expect the CNL to be in close proximity with the LUMO so that injected carriers

will not have the tendency to relax to the interfacial trap states. Electron injection into the CoP^{1-} states to become a dianion (CoP^{2-}) is not favorable until the LUMO energy is one $\Delta E_{\mathrm{ch},e}$ below the silicon conduction band edge, which corresponds to the 5-eV blockade voltage at room temperature. Sequential electron injection can be stable in the orbital states, as long as the leakage back to the substrate is not severe. The single-electron charging energy can be calculated by

$$\Delta E_{\mathrm{ch},e} = \frac{q^2}{C} \tag{4}$$

where C is the self-capacitance of the storage node. However, the charging energy can only be estimated using a detailed calculation considering the complex geometry of the redox molecule embedded in the dielectric, which is not performed here. Instead, we will calculate the charging energy by first determining the self-capacitance by the following relation:

$$C_{\mathrm{self}} = C_{\mathrm{CoP}} \times A_{\mathrm{CoP}} \tag{5}$$

where C_{self}, C_{CoP}, and A_{CoP} are the self-capacitance, the capacitance per unit area, and the areal coverage of each CoP molecule, respectively. The capacitance per unit area can be extracted from impedance spectroscopy, which is 1.5 μF/cm^2 for the device with CoP molecules, estimated from previous literature [8]. A_{CoP} is estimated from the amount of ΔV_{FB}, which separates each reduced states.

In Fig. 10, the amount of ΔV_{FB} between the plateau regions is ~1.5 V at 10 K. In (2), we calculate the number density N to be 2.5×10^{12} cm^{-2}, which translates to the unit cell area A_{cell} of 4×10^{-13} cm^2. Assuming a close-packed SAM and the mixture ratio in a liquid solution to be the same as the as-deposited molecules, the areal coverage of each CoP molecule A_{CoP} is 2×10^{-14} cm^2, which can be calculated by the relation $A_{\mathrm{cell}}/A_{\mathrm{CoP}} \sim 20$, considering the mixture ratio of 1:20 with H_2P. In (5), the self-capacitance of the CoP molecule can be readily calculated to be 3×10^{-20} F.

In (4), the single-electron charging energy $\Delta E_{\mathrm{ch},e}$ can be calculated to be ~5.6 eV. The ε_M, t_m, and t_M values for the CoP SAM are 2.5, 0.8 nm, and 1.6 nm, respectively. The t_{tunn} of the heterogeneous tunneling oxide is 2.7 nm. With these molecular parameters, the first plateau region in Fig. 10 has a blockade voltage of ~5.3 eV at 10 K by (3), which is in good agreement with the single-electron charging energy of the CoP molecule (5.6 eV).

Finally, Fig. 12 shows the programming and retention characteristics for FcCOOH and CoP molecules. The retention time t_R/programming time t_P ratio of the device with CoP molecules is clearly improved compared with the device with FcCOOH molecules as the storage node, possibly due to the large capture cross section of the redox molecules in comparison with the interfacial trap states in the device with FcCOOH molecules. Further improvement on program efficiency, voltage operation, and retention is possible by adjusting the oxide thickness ratio, tunnel oxide thickness, and surface coverage density of the molecules; integrating different redox molecules with various orbital energy levels; and improving the dielectric quality.

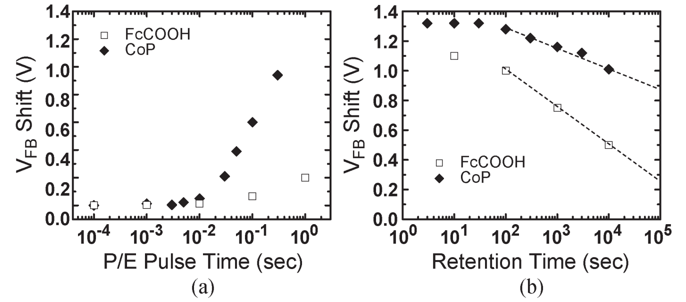

Fig. 12. (a) Programming and (b) retention measurements of MOS capacitors with FcCOOH and CoP molecules. ΔV_{FB} was extracted from HFCV measurements. Devices were stressed for 5 s at +10 V before the retention measurement and programming tests were applied at +10 V. The sample with FcCOOH molecules has a tunneling oxide of 3-nm thermally grown SiO_2, and a 60-min forming gas anneal was performed at 200 °C. The mixture ratio between FcCOOH and Bz is 1 : 200. The sample with CoP molecules has a heterogeneous tunnel oxide composed of 1.4-nm native SiO_2 and 3-nm plasma ALD Al_2O_3.

IV. Conclusion

We have successfully integrated a monolayer of redox molecules in a Flash memory device structure using a solution-based self-assembly technique and demonstrated three programmable MO states of the CoP molecule, including CoP^0, CoP^{1-}, and CoP^{2-}, at room temperature, which may help realize step charging into a multibit memory cell. For the device with FcCOOH molecules, the memory window increases proportionally with the density of the redox molecules, and the band offset of the HOMO–LUMO energy levels of FcCOOH molecules and the CNL of Al_2O_3 determines the preferred carrier storage sites. With the abundant choices of redox molecules and their inherent monodispersion in size and energy levels, our proposed approach can be readily integrated into a MOS-based nonvolatile memory cell and pave the wave for realizing multilevel molecular memory devices. Furthermore, mixture of porphyrins with different transitional metals or integration of multistate molecules [23] may offer additional MO states while maintaining a small bit error rate.

References

[1] T.-H. Hou, C. Lee, V. Narayanan, U. Ganguly, and E. C. Kan, "Design optimization of metal nanocrystal memory—Part II: Gate-stack engineering," *IEEE Trans. Electron Devices*, vol. 53, no. 12, pp. 3103–3109, Dec. 2006.

[2] C. Lee, U. Ganguly, V. Narayanan, T.-H. Hou, and E. C. Kan, "Asymmetric electric field enhancement in nanocrystal memories," *IEEE Electron Device Lett.*, vol. 26, no. 12, pp. 879–881, Dec. 2005.

[3] L. Perniola, B. De Salvo, G. Ghibaudo, A. F. Para, G. Pananakakis, V. Vidal, T. Baron, and S. A. Lombardo, "Modeling of the programming window distribution in multi-nanocrystal memory," *IEEE Trans. Nanotechnol.*, vol. 2, no. 4, pp. 277–284, Dec. 2003.

[4] J. T. Shaw, T.-H. Hou, H. Raza, and E. C. Kan, "Statistical metrology of metal nanocrystal memories with 3-D finite-element analysis," *IEEE Trans. Electron Devices*, vol. 56, no. 8, pp. 1729–1735, Aug. 2009.

[5] T.-H. Hou, U. Ganguly, and E. C. Kan, "Programmable molecular orbital states of C_{60} from integrated circuits," *Appl. Phys. Lett.*, vol. 89, no. 25, pp. 253 113-1–253 113-3, Dec. 2006.

[6] Q. Li, S. Surthi, G. Mathur, G. Gowda, T. A. Sorenson, R. C. Tenent, W. G. Kuhr, S.-I. Tamaru, J. S. Lindsey, Z. Liu, D. F. Bocian, and V. Misra, "Electrical characterization of redox-active molecular monolayers on SiO_2 for memory applications," *Appl. Phys. Lett.*, vol. 83, no. 1, pp. 198–200, Jun. 2003.

[7] Q. Li, G. Mathur, M. Homsi, S. Surthi, V. Misra, V. Malinovskii, K. H. Schweikart, L. H. Yu, J. S. Lindsey, Z. M. Liu, R. B. Dabke, A. Yasseri, D. F. Bocian, and W. G. Kuhr, "Capacitance and conductance

characterization of ferrocene-containing self-assembled monolayers on silicon surfaces for memory applications," *Appl. Phys. Lett.*, vol. 81, no. 8, pp. 1494–1496, Aug. 2002.
[8] Q. Li, "Approach towards hybrid silicon/molecular electronics for memory applications," in *Electrical and Computer Engineering*. Raleigh, NC: North Carolina State Univ., 2004, p. 152.
[9] G. Mathur, S. Gowda, Q. Li, S. Surthi, Q. Zhao, and V. Misra, "Properties of functionalized redox-active monolayers on thin silicon dioxide—A study of the dependence of retention time on oxide thickness," *IEEE Trans. Nanotechnol*, vol. 4, no. 2, pp. 278–283, Mar. 2005.
[10] S. Kubatkin, A. Danilov, M. Hjort, J. Cornil, J.-L. Bredas, N. Stuhr-Hansen, P. Hedegard, and T. Bjornholm, "Single-electron transistor of a single organic molecule with access to several redox states," *Nature*, vol. 425, no. 6959, pp. 698–701, Oct. 2003.
[11] Z. Liu, A. A. Yasseri, J. S. Lindsey, and D. F. Bocian, "Molecular memories that survive silicon device processing and real-world operation," *Science*, vol. 302, no. 5650, pp. 1543–1545, Nov. 2003.
[12] C. Lee, J. Meteer, V. Narayanan, and E. C. Kan, "Self-assembly of metal nanocrystal on ultra-thin oxide for nonvolatile memory applications," *J. Electron. Mater.*, vol. 34, no. 1, pp. 1–11, Jan. 2005.
[13] T.-H. Hou, U. Ganguly, and E. C. Kan, "Fermi-level pinning in nanocrystal memories," *IEEE Electron Device Lett.*, vol. 28, no. 2, pp. 103–106, Feb. 2007.
[14] A. S. Killampalli, P. F. Ma, and J. R. Engstrom, "The reaction of tetrakis(dimethylamido)-titanium with self-assembled alkyltrichlorosilane monolayers possessing –OH, $-NH_2$, and $-CH_3$ terminal groups," *J. Am. Chem. Soc.*, vol. 127, no. 17, pp. 6300–6310, May 2005.
[15] N. W. Ashcroft and N. D. Mermin, *Solid State Physics*. Fort Worth, TX: Harcourt Brace College, 1976.
[16] C. J. Powell and A. Jablonski, "Consistency of calculated and measured electron inelastic mean free paths," *J. Vac. Sci. Technol. A.*, vol. 17, no. 4, pp. 1122–1126, Jul. 1999.
[17] J. H. Scofield, "Hartree–Slater subshell photoionization cross-sections at 1254 and 1487 eV," *J. Electron Spectrosc.*, vol. 8, no. 2, pp. 129–137, 1976.
[18] M. G. Grigorov, J. Weber, N. Vulliermet, H. Chermette, and J. M. J. Tronchet, "Numerical evaluation of the internal orbitally resolved chemical hardness tensor: Second order chemical reactivity through thermal density functional theory," *J. Chem. Phys.*, vol. 108, no. 21, pp. 8790–8798, Jun. 1998.
[19] M.-S. Liao and S. Scheiner, "Electronic structure and bonding in metal porphyrins, metal = Fe, Co, Ni, Cu, Zn," *J. Chem. Phys.*, vol. 117, no. 1, pp. 205–219, Jul. 2002.
[20] S. B. Samavedam, L. B. La, P. J. Tobin, B. White, C. Hobbs, L. R. C. Fonseca, A. A. Demkov, J. Schaeffer, E. Luckowski, A. Martinez, M. Raymond, D. Triyoso, D. Roan, V. Dhandapani, R. Garcia, S. G. H. Anderson, K. Moore, H. H. Tseng, C. Capasso, O. Adetutu, D. C. Gilmer, W. J. Taylor, R. Hegde, and J. Grant, "Fermi level pinning with sub-monolayer MeOx and metal gates," in *IEDM Tech. Dig.*, 2003, pp. 13.1.1–13.1.4.
[21] J. Tersoff, "Theory of semiconductor heterojunctions: The role of quantum dipoles," *Phys. Rev. B*, vol. 30, no. 8, pp. 4874–4877, Oct. 1984.
[22] S. Lenfant, D. Guerin, F. Tran Van, C. Chevrot, S. Palacin, J. P. Bourgoin, O. Bouloussa, F. Rondelez, and D. Vuillaume, "Electron transport through rectifying self-assembled monolayer diodes on silicon: Fermi-level pinning at the molecule–metal interface," *J. Phys. Chem.*, vol. 110, no. 28, pp. 13 947–13 958, Jul. 2006.
[23] D. Gryko, J. Z. Li, J. R. Diers, K. M. Roth, D. F. Bocian, W. G. Kuhr, and J. S. Lindsey, "Studies related to the design and synthesis of a molecular octal counter," *J. Mater. Chem.*, vol. 11, no. 4, pp. 1162–1180, Feb. 2001.

Jonathan Shaw received the B.S. degree in electrical engineering from the University of California, San Diego, La Jolla, in 2006. He is currently working toward the Ph.D. degree with the School of Electrical and Computer Engineering, Cornell University, Ithaca, NY.

His current research interests include nanocrystal and molecular-based memory devices.

Yu-Wu Zhong received the Ph.D. degree from the Chinese Academy of Sciences, Beijing, China, in 2004, under the supervision of Prof. G.-Q. Lin.

He was a Postdoctoral Associate with Prof. E. Nakamura at the University of Tokyo, Tokyo, Japan, from 2004 to 2006 and with Prof. H. D. Abruña at Cornell University, Ithaca, NY, from 2006 to 2009. He is currently a Professor with the Laboratory of Photochemistry, Institute of Chemistry, Chinese Academy of Sciences. His research interests include the synthesis of functional organometallic materials and their application for molecular electronics and photovoltaics.

Kevin J. Hughes received the B.S. degree in chemical engineering from Carnegie Mellon University, Pittsburgh, PA, in 2003. He is currently working toward the Ph.D. degree with the School of Chemical and Biomolecular Engineering, Cornell University, Ithaca, NY. His thesis research involves the growth of inorganic materials on thin organic layers using atomic layer deposition.

He spent two years as a Research Engineer with Lubrizol Corporation.

Tuo-Hung Hou received the B.S. and M.S. degrees from National Chiao Tung University, Hsinchu, Taiwan, in 1996 and 1998, respectively, and the Ph.D. degree from Cornell University, Ithaca, NY, in 2008, all in electrical engineering.

From 1998 to 2000, he served as a Second Lieutenant in the Taiwanese Army. In April 2000, he joined the Advanced Module Technology Division, Taiwan Semiconductor Manufacturing Company (TSMC), where he worked in the area of deep-submicrometer front-end process development. From 2001 to 2003, he was also a TSMC Assignee with the International Semiconductor Manufacturing Technology, Austin, TX, engaged in high-κ gate dielectric research for two years. He is currently an Assistant Professor with the School of Electrical and Computer Engineering, National Chiao Tung University. His current research interests include novel devices by nanocrystal and nanotube integration.

Hassan Raza (M'07) received the B.S. degree (with honors) from the University of Engineering and Technology, Lahore, Pakistan, in 2001 and the M.S. and Ph.D. degrees from Purdue University, West Lafayette, IN, in 2002 and 2007, respectively, all in electrical engineering.

In May 2007, he joined the Center for Nanoscale Systems, Cornell University, Ithaca, NY, as a Postdoctoral Associate. He is currently an Assistant Professor with the College of Engineering, University of Iowa, Iowa City. His research interests include the experimental, theoretical, and computational aspects of quantum transport for novel logic and memory devices in various material systems, e.g., graphene, carbon nanotubes, molecules, and quantum dots.

Dr. Raza was a recipient of the Magoon Award for Excellence in Teaching from Purdue University in 2004 and the Presidential Faculty Fellowship of the University of Iowa in 2010.

Shantanu Rajwade received the B.Tech. degree in electrical engineering and the M.Tech. degree in microelectronics from the Indian Institute of Technology, Mumbai, India, in 2007. He is currently working toward the Ph.D. degree in electrical and computer engineering with Cornell University, Ithaca, NY.

His research interests include device physics, nanoscale carrier transport, low-power logic and memory devices, and their applications to nonvolatile computing in future embedded system-on-a-chip platforms.

Julie Bellfy is currently working toward the B.S. degree in chemical engineering with Villanova University, Villanova, PA.

Her current research interests include metal–oxide–semiconductor capacitors, thin films, and monolayers.

James R. Engstrom received the B.S. degree in chemical engineering from the University of Minnesota, Minneapolis, in 1981 and the Ph.D. degree in chemical engineering from the California Institute of Technology, Pasadena, in 1987.

From 1998 to 2001, he was with Symyx Technologies, as the Director and, eventually, the Vice President of High-Throughput Screening and Electronic Materials, where he spearheaded the development of new technologies for high-throughput screening. In 2001, he joined Cornell University, Ithaca, NY. Since 2002, he has been a member of the Graduate Field of Chemistry and Chemical Biology, Cornell University. He is currently the B. P. Amoco/H. Laurance Fuller Professor with the School of Chemical and Biomolecular Engineering, Cornell University. He is the author of more than 70 peer-reviewed publications and has presented his work at more than 180 national and international meetings, as well as to private industry. He is the holder of ten patents. He is widely recognized for his work concerning supersonic molecular beam scattering of thin-film precursors from semiconductor surfaces and fundamental studies of thin-film deposition, making use of precisely controlled beams of molecular and/or atomic species, with applications in silicon-based microelectronics. His current research focuses on two areas, namely, inorganic–organic interfaces and organic thin-film electronics. Concerning the former, he is actively engaged in research that seeks to build robust interfaces between organic thin films/monolayers and inorganic (dielectric or metallic) thin-film overlayers. This topic has applications in the areas of molecular electronics and barrier layers for microelectronics interconnect and packaging. Concerning the latter, his group is currently aggressively pursuing fundamental studies of small-molecule organic thin films, such as pentacene. In this work, in addition to using molecular-beam-based techniques, his group is also making use of real-time *in situ* X-ray scattering that gives unprecedented information concerning the dynamics of growth.

Dr. Engstrom is a Fellow of the American Vacuum Society. He was a recipient of numerous awards, including the National Science Foundation Presidential Young Investigator Award and two College of Engineering Teaching Awards.

Héctor D. Abruña received the Ph.D. degree, with R. W. Murray and T. J. Meyer, from the University of North Carolina at Chapel Hill in 1980.

He was a Postdoctoral Research Associate with A. J. Bard at the University of Texas at Austin. After a brief stay at the University of Puerto Rico, San Juan, Puerto Rico, in 1983, he joined Cornell University, Ithaca, NY, where he is currently an Emile M. Chamot Professor of Chemistry.

Prof. Abruña is a Fellow of the American Association for the Advancement of Science. He was a recipient of the Presidential Young Investigator Award, the Alfred P. Sloan Foundation Research Fellowship, the John S. Guggenheim Fellowship, the Tajima Prize of the International Society of Electrochemistry, the J. W. Fulbright Senior Research Fellowship, and the Iberdrola Fellowship.

Edwin Chihchuan Kan (S'86–M'91–SM'05) received the B.S. degree from National Taiwan University, Taipei, Taiwan, in 1984 and the M.S. and Ph.D. degrees from the University of Illinois at Urbana-Champaign in 1988 and 1992, respectively, all in electrical engineering.

In January 1992, he joined Dawn Technologies as a Principal Computer-Aided Design (CAD) Engineer, developing advanced electronic and optical device simulators and technology CAD frameworks. From 1994 to 1997, he was with Stanford University, Palo Alto, CA, as a Research Associate. From 1997 to 2002, he was an Assistant Professor with the School of Electrical and Computer Engineering, Cornell University, Ithaca, NY, where he is currently a Professor. He spent the summers of 2000 and 2001 at IBM Microelectronics, Yorktown Heights and Fishkill, NY, in the Faculty Partner Program. In 2004 and 2005, he was a Visiting Researcher with Intel Research, Santa Clara, CA, and a Visiting Professor with Stanford University during his sabbatical leave. His main research areas include complementary metal–oxide–semiconductor (CMOS) technology, semiconductor device physics, Flash memory, CMOS sensors, ultralow-power radio link, composite CAD, and numerical methods for partial and ordinary differential equations.

Dr. Kan was a recipient of the Presidential Early Career Award for Scientists and Engineer in October 2000 from the White House, as well as several teaching awards from Cornell Engineering College for his CMOS and microelectromechanical system courses.